Article

Chinese Science Bulletin

Atmospheric Science

June 2013 Vol.58 No.16: 1948–1954
doi: 10.1007/s11434-012-5652-7

Incorporating temporal variability to improve geostatistical analysis of satellite-observed CO_2 in China

ZENG ZhaoCheng[1,2], LEI LiPing[1*], GUO LiJie[1,2], ZHANG Li[1] & ZHANG Bing[1]

[1] *Key Laboratory of Digital Earth Science, Center for Earth Observation and Digital Earth, Chinese Academy of Sciences, Beijing 100094, China;*
[2] *University of Chinese Academy of Sciences, Beijing 100049, China*

Received July 30, 2012; accepted November 23, 2012; published online January 10, 2013

Observations of atmospheric carbon dioxide (CO_2) from satellites offer new data sources to understand global carbon cycling. The correlation structure of satellite-observed CO_2 can be analyzed and modeled by geostatistical methods, and CO_2 values at unsampled locations can be predicted with a correlation model. Conventional geostatistical analysis only investigates the spatial correlation of CO_2, and does not consider temporal variation in the satellite-observed CO_2 data. In this paper, a spatiotemporal geostatistical method that incorporates temporal variability is implemented and assessed for analyzing the spatiotemporal correlation structure and prediction of monthly CO_2 in China. The spatiotemporal correlation is estimated and modeled by a product-sum variogram model with a global nugget component. The variogram result indicates a significant degree of temporal correlation within satellite-observed CO_2 data sets in China. Prediction of monthly CO_2 using the spatiotemporal variogram model and space-time kriging procedure is implemented. The prediction is compared with a spatial-only geostatistical prediction approach using a cross-validation technique. The spatiotemporal approach gives better results, with higher correlation coefficient (r^2), and less mean absolute prediction error and root mean square error. Moreover, the monthly mapping result generated from the spatiotemporal approach has less prediction uncertainty and more detailed spatial variation of CO_2 than those from the spatial-only approach.

CO_2, Greenhouse Gases Observing Satellite (GOSAT), geostatistical analysis, space-time kriging, product-sum model

Citation: Zeng Z C, Lei L P, Guo L J, et al. Incorporating temporal variability to improve geostatistical analysis of satellite-observed CO_2 in China. Chin Sci Bull, 2013, 58: 1948–1954, doi: 10.1007/s11434-012-5652-7

As one of the long-lived greenhouse gases, carbon dioxide (CO_2) contributes greatly to global warming [1,2]. With global coverage and high measurement density, satellite observations of CO_2 provide new ways to understand the functioning of the carbon cycle [3]. Although observing at high density, these satellite observations have gaps and are irregularly positioned because of certain limitations, such as cloud and the observational mode of the satellite [4]. Filling the gaps and analyzing global and regional characteristics of CO_2 are required to study sources and sinks of CO_2. Geostatistical analysis can be used to meet this requirement, since geostatistical methods use the inherent autocorrelation between satellite-observed CO_2 data points. Further, the methods for handling the irregular data are flexible. Geostatistical study includes two main parts: investigation of the correlation structure of the data via variogram analysis, and optimum prediction (kriging) of the variable at gap locations.

Conventional spatial-only geostatistical analysis, which only investigates spatial correlation, has been done in several studies of satellite-observed CO_2 [5–8]. However, the spatial-only approach ignores the temporal structure of the data; the dynamic CO_2 variation has not only a zonal variable distribution but also a yearly trend and seasonal cycle [9]. The CO_2 temporal variability can be used in the geostatistical analysis of satellite-observed CO_2. The satellite-observed CO_2 data product can include temporal variability information, since the orbital period of the satellite is sufficiently short, e.g. 3 d for the Greenhouse Gases Observing Satellite (GOSAT). Geostatistical analysis can be improved when the spatial and temporal correlation structures of the

*Corresponding author (email: lplei@ceode.ac.cn)

satellite-observed CO_2 are used to support model estimation and location-specific prediction. In this paper, a spatiotemporal geostatistical method that incorporates both spatial and temporal variability is implemented for analysis of the spatiotemporal correlation structure and prediction of monthly CO_2 in China. Improvement produced by the method is verified by comparing to the spatial-only geostatistical method, with respect to accuracies and uncertainty of prediction.

1 Data and methods

1.1 Data used and study area

We used data derived from observations of GOSAT, which was launched on January 23, 2009. It is the first spacecraft designed to measure concentrations of the two major greenhouse gases, CO_2 and methane, from space [10]. GOSAT Level 2 data are CO_2 dry air mixing ratios (XCO_2), defined by the ratio of total number of CO_2 molecules to that of dry molecules, not only near the earth surface but also in the entire vertical column to the top of atmosphere [4]. Version 2.0 of the GOSAT Level 2 data product was released in April 2012. Validation results [11] indicated that GOSAT Level 2 XCO_2 values were smaller than those from the Total Carbon Column Observing Network data by 0.3% (1.2 ppm), and standard deviation of the Level 2 XCO_2 data was 0.5% (2.0 ppm). We collected the GOSAT version 2.0 Level 2 data product released for Research Announcement (RA) users from June 2009 to May 2010, during which 10367 observations were available. The data process flow including data screening conditions of RA data products is described in [12].

The study area extends from latitude 21° to 54°N and longitude 70° to 138°E, covering the Chinese mainland. Data of sea and islands were excluded because the greenhouse gas tendency largely varies between land and sea, causing a difference in their empirical variograms [6]. The study area and data used from April 2010 are shown as an example in Figure 1.

The full set of CO_2 data from June 2009 to May 2010 was divided into 12 monthly data sets by observation date. Basic summary statistics of these data sets are given in Table 1. The mean value for August was the smallest, and April the largest. Variations of the monthly data, indicated by the standard deviation, were nearly identical.

1.2 Geostatistical methods

Implementation of the spatial-only geostatistical method for analyzing spatially correlated data is well documented in the literature [13,14] Spatiotemporal geostatistical analysis of data is less common, but has increased in recent years [15–17]. The extension of spatial-only geostatistical techniques to the space-time domain is not straightforward, since the behavior of a variable over time differs from its behavior over space. For example, periodic variation over time with daily or season patterns is common, whereas periodic variation in space is less common. A brief introduction of spatial-only geostatistical methods is furnished in this section, followed by introduction of the spatiotemporal geostatistical model and methods for analysis of satellite-observed CO_2.

(i) Spatial-only geostatistical analysis. For the conventional, spatial-only geostatistical analysis of satellite-observed CO_2, a set of spatial CO_2 data denoted by the variable $z=\{z(s)|s\in S\}$ is considered. z varies within a spatial domain S, and we let z be observed at m space points s_i, $i=1,\cdots, m$. The

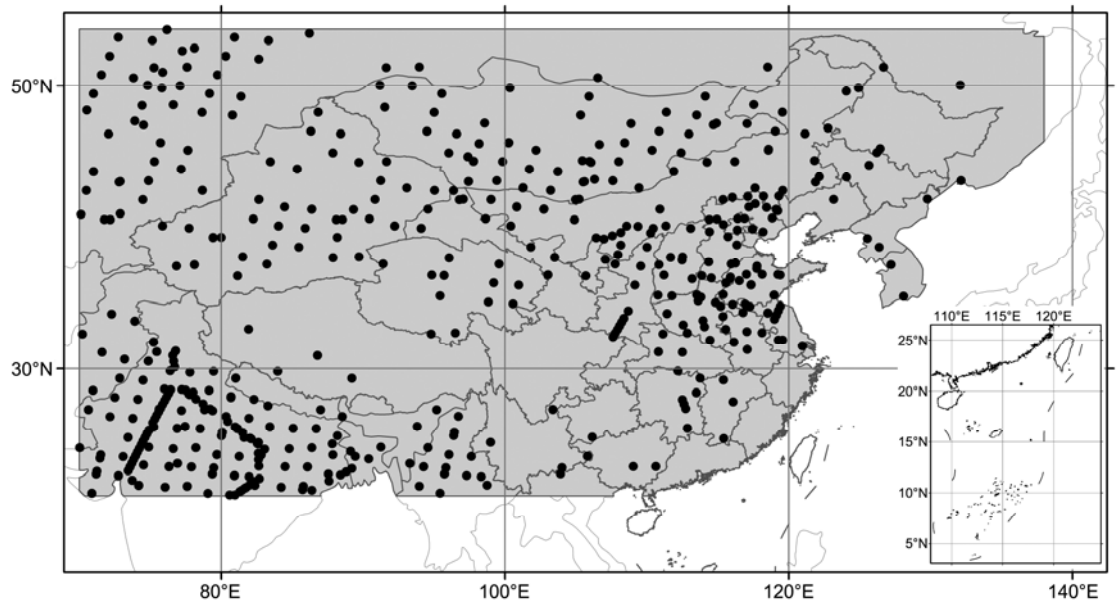

Figure 1 Example of spatial distribution of GOSAT v2.0 data (black dots) from April 2010 across study area (gray color).

Table 1 Basic summary statistics of GOSAT Level 2 XCO_2 data used

		XCO_2				
		Number of observations	Minimum (ppm)	Maximum (ppm)	Mean (ppm)	Standard deviation
2009	June	553	374.24	391.53	382.40	2.96
	July	397	369.84	394.53	379.31	3.12
	August	553	368.58	389.02	378.19	2.78
	September	983	369.42	388.11	380.14	2.62
	October	1789	372.77	392.51	382.08	2.38
	November	968	373.20	394.62	384.43	2.49
	December	954	367.47	399.59	385.84	2.86
2010	January	1000	375.10	399.37	387.24	3.11
	February	732	381.06	397.01	387.62	2.65
	March	1017	375.89	404.06	388.97	2.89
	April	837	381.72	399.79	389.39	2.89
	May	584	380.85	398.96	388.55	2.70

objective for the standard geostatistical problem is to obtain a prediction of $z(s_0)$ at a point s_0 where z was not observed using the geostatistical prediction method; this is also called kriging. Along with data, kriging predictors also require estimation of the variogram between z data separated by different lags, and fitting a variogram model to the variogram estimation. The model can provide a variogram value at any given lag for input into the kriging process [13]. This traditional spatial-only method has been recently extended to incorporate data distributed in both space and time [15], and has been developed into the spatiotemporal geostatistical method.

(ii) Spatiotemporal geostatistical modeling and analysis. The spatiotemporal variation of CO_2 can be represented by considering a variable $Z=\{Z(s,t)\,|\,s\in S,\ t\in T\}$ that varies within a spatial domain S and time interval T. We let Z be observed at n space-time points (s_i,t_i), i=1,…, n. The space-time variation of Z can be characterized using a general model, given by

$$Z(s,t)=m(s,t)+R(s,t), \tag{1}$$

where $m(s,t)$ is a deterministic space-time component that models the trend. $R(s,t)$ is the residual component that denotes an intrinsically stationary space-time error process. As described in a World Meteorological Organization report [1], CO_2 has a non-constant spatial trend as well as a temporal trend. The latter consists of a seasonal component and yearly trend. The trend component can be described by a linear trend surface plus a set of annual harmonic functions [9,18], as

$$m(s,\ t)=[a_0+a_1\times s(1)+a_2\times s(2)]+\left[a_3\times t+\sum_{i=1}^{4}\left(\beta_i\sin(i\omega t)+\gamma_i\cos(i\omega t)\right)\right], \tag{2}$$

where $\omega=\dfrac{2\times\pi}{12}$ since the period is 12 months, $s(1)$ and $s(2)$ are latitude and longitude of the spatial location, t is time in months, and a_{0-3}, β_{0-4} and γ_{0-4} are parameters to be estimated. The estimated spatiotemporal trend component is then subtracted from the full dataset to yield the spatiotemporal residuals $R(s,t)$. Spatiotemporal geostatistical methods are concerned with analyzing the spatial-temporal correlation structure of regional variables using the variogram, and optimal prediction of the value of the variable at an unsampled location and time. An experimental variogram at spatial lag h_s and temporal lag h_t, $2\hat{\gamma}(h_s,h_t)$, is computed by

$$2\hat{\gamma}(h_s,h_t)=\frac{1}{N(h_s,h_t)}\sum_{N(h_s,h_t)}\left[R(s,t)-R(s+h_s,t+h_t)\right]^2, \tag{3}$$

where $N(h_s,h_t)$ is the number of pairs in the space and time lags. Half of a variogram quantity, $\hat{\gamma}(h_s,h_t)$, has been called a semi-variance. Once the experimental variogram has been constructed, a spatiotemporal variogram model, $\gamma(h_s,h_t)$, is fitted to it. The choice of variogram model and estimation of model parameters are the critical stages in the prediction process. The spatiotemporal variogram model adopted here is a combination of the product-sum model [19–21] and an extra global nugget N_{ST} to capture the nugget effect [13], and is given by

$$\gamma(h,u)=\gamma_S(h)+\gamma_T(u)-\kappa\cdot\gamma_S(h)\gamma_T(u)+N_{ST}, \tag{4}$$

where $\gamma_S(h)$ and $\gamma_T(u)$ are the marginal spatial and temporal variograms, and κ is a constant in need of estimation. All parameters are estimated simultaneously to overcome the limitation of conventional product-sum fitting [22]. The nonlinear, weighted least square estimation technique [23] was used for parameter calculation. The subsequent prediction procedure is known as space-time kriging. Kriging yields the best linear unbiased predictor of $R(s_0,t_0)$ as

$$\hat{R}(s_0,t_0)=\sum_{i=1}^{n}\left[\lambda_i R(s_i,\ t_i)\right], \tag{5}$$

where λ_i is the weight assigned to a known sample $R(s_i,t_i)$ so as to minimize the prediction variance while maintaining unbiasedness of the predictor. The prediction variance is given by

$$\sigma^2=\gamma_0{}^T\Gamma^{-1}\gamma_0-\frac{\left(1^T\boldsymbol{\Gamma}^{-1}\gamma_0-1\right)^2}{1^T\boldsymbol{\Gamma}^{-1}1}, \tag{6}$$

where $\boldsymbol{\Gamma}(i,j)=\gamma(|s_i-s_j|,|t_i-t_j|)$, $\gamma_0(i,1)=\gamma(|s_i-s_0|,|t_i-t_0|)$, and 1 is $n\times1$ unit vector. To reduce computational complexity and preserve local variability, data used in the prediction were searched within an appropriate spatiotemporal neighborhood centered on the predicting point [17]. As in [6], the predicting position is maintained as a missing value if no more than 20 data are found within the neighborhood.

1.3 Evaluation of methods

Cross-validation is effective and widely used for assessing model prediction [24], and it can be used to compare and assess prediction accuracies between spatial-only and space-time kriging [20,21,25]. As above, we considered a set of data denoted by the variable $Z=\{Z(s,t)\mid s\in S,\ t\in T\}$ that varies within a spatial domain S and time interval T. We let Z be observed at n space-time points (s_i,t_i), $i=1,\cdots,n$. Cross-validation proceeds by removing an original observation datum $Z(s_j,\ t_j)$ and then making its prediction $\hat{Z}(s_j,t_j)$ at this point, using the kriging prediction mentioned above. This process is repeated for each observation in the dataset. After all the original data were manipulated, we obtained two data sets, the predicted data set $\{\hat{Z}(s_j,t_j)\ j=1\cdots n.\}$ and corresponding original data set $\{Z(s_j,t_j)\ j=1\cdots n.\}$. Three summary statistics of cross-validation were derived to assess prediction precision: the correlation coefficient (r^2) between these two data sets, mean absolute prediction error (MAE), and root mean square error (RMSE). The latter two statistics are defined by

$$\mathrm{MAE}=\frac{1}{n}\sum_{j=1}^{n}\left|Z(s_j,t_j)-\hat{Z}(s_j,t_j)\right|, \tag{7}$$

$$\mathrm{RMSE}=\sqrt{\frac{1}{n}\sum_{j=1}^{n}\left[Z(s_j,t_j)-\hat{Z}(s_j,t_j)\right]^2}. \tag{8}$$

r^2 provides a straightforward measure of linear association between the predictions and observations, and MAE measures bias of the mean accuracy of individual prediction. Both MAE and RMSE measure model accuracy and smaller values for these two statistics are assumed to indicate better performance.

2 Results and discussion

2.1 Variogram

(i) Spatial-only variograms. Figure 2 shows monthly experimental spatial variograms estimated using spatial-only geostatistics for all 12 months in the dataset, and corresponding fitted variogram models. The fitted variogram model is an exponential model with a nugget-effect component, given by

$$\gamma(L)=N+C\times\left(1-\exp\left(-L/R\right)\right), \tag{9}$$

where N is the nugget-effect component, C is the sill value, R is the range value, and L represents the distance lags in space. As indicated by these variograms, their structure was consistent across the 12 experimental variograms, which supports the use of the sample class of variogram model in eq. (9). The estimated range, sill and nugget parameter values, however, displayed considerable variation between months.

(ii) Spatiotemporal variograms. Figure 3 shows the experimental spatiotemporal variogram surface of the residuals component and its fitted model. As indicated by the variogram, the CO_2 observations had significant spatial and temporal correlation, and the temporal marginal variogram differed substantially in structure from the spatial marginal variogram.

A potential advantage of spatiotemporal geostatistical analysis is that incorporation of temporal variability provided more data for stable variogram estimation. It was expected that the prediction based on the spatiotemporal variogram was made more accurate by exploiting the temporal structure and allowing the use of data in both space and time domains. Furthermore, the spatiotemporal approach was less labor-intensive, because it required estimation and modeling of a single spatiotemporal variogram rather than 12 separate spatial variograms in the spatial-only approach.

2.2 Comparison of prediction accuracies

To access and compare prediction accuracies between the spatial-only and spatiotemporal approaches, the cross-validation technique was applied to the data using a two-prediction approach, and the three summary statistics (r^2, MAE and RMSE) were calculated for the 12 months. The results are shown in Table 2.

As expected, all correlation coefficients for the spatiotemporal approach were greater than those for the spatial-only approach, indicating a stronger linear correlation between CO_2 observations and the predicted set for the spatiotemporal geostatistical prediction. Furthermore, all the smaller RMSEs and MAEs were produced by the spatiotemporal approach, signifying a more precise prediction. It is concluded from these three statistics that the latter approach outperformed the spatial-only approach in prediction precision.

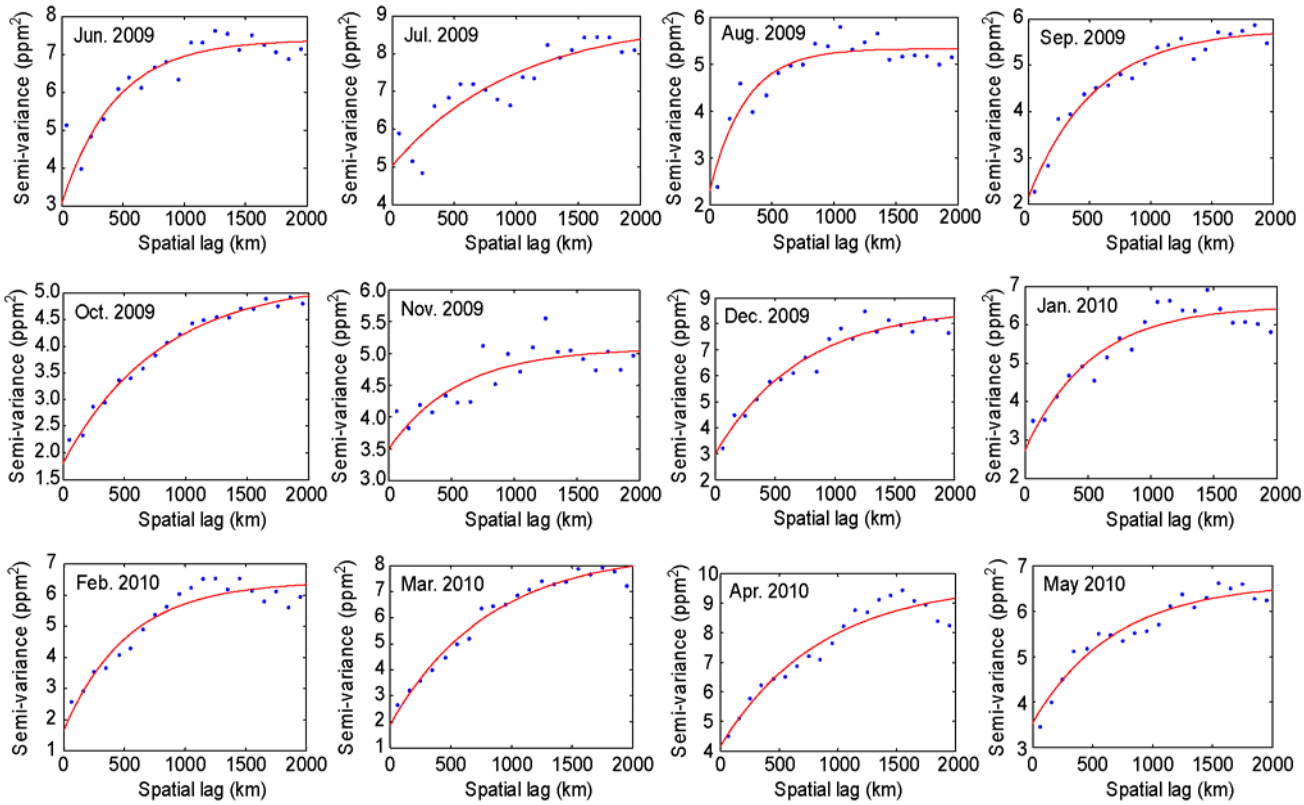

Figure 2 Monthly experimental spatial variograms (dots) estimated using spatial-only geostatistics for all 12 months in dataset, and corresponding fitted variogram models (red lines).

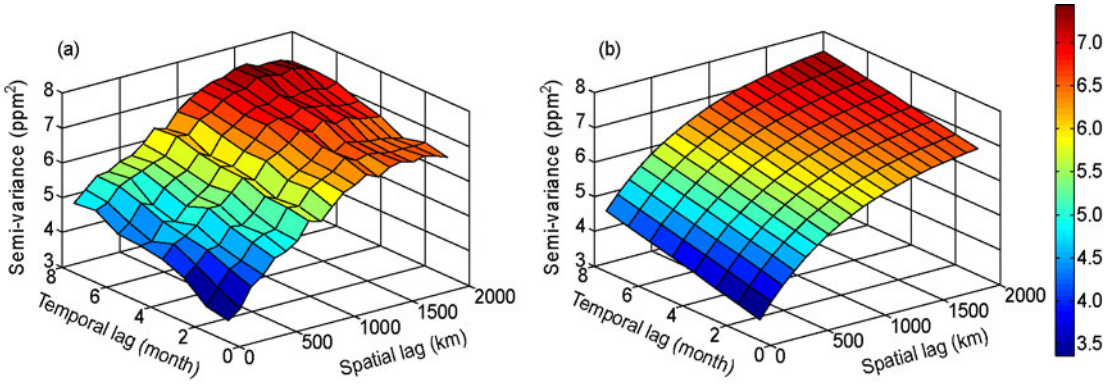

Figure 3 Spatiotemporal variogram for satellite-observed CO_2 in China. (a) Spatiotemporal experimental variogram, and (b) its fitted variogram model.

2.3 Mapping result for China

We took the map of CO_2 prediction for April as an example, as shown in Figure 4(a) and (b). Overall spatial variations of CO_2 in the two maps were in general agreement. The prediction map from the spatiotemporal approach, however, yielded more detailed variability on the small scale. This is because more satellite-observed CO_2 data, proximate in space and time, were used for prediction.

In geostatistical mapping, each predicted CO_2 value is accompanied by a prediction variance (eq. (6)) that quantifies the prediction uncertainty. In general, a more homogeneous area with dense observations results in lower prediction uncertainty [8,26]. Corresponding maps of prediction standard deviation (root prediction variance) in April are shown in Figure 5(a) and (b). Comparison of the two maps shows that the spatiotemporal approach produced a much lower prediction uncertainty (average prediction standard deviation 1.99 ppm) than the spatial-only approach (average prediction standard deviation 2.40 ppm). From the maps, a reasonable distribution of prediction standard deviation can be inferred that areas with more data points (Figure 1) generated less prediction uncertainty.

Compared to the spatial-only prediction approach, there

Table 2 Cross-validation summary statistics of 12 months, for spatial-only and spatiotemporal geostatistical prediction approaches

		Spatial-only			Spatiotemporal		
		r^2	RMSE (ppm)	MAE (ppm)	r^2	RMSE (ppm)	MAE (ppm)
2009	June	0.57	2.27	1.80	0.62	2.18	1.77
	July	0.59	2.45	1.94	0.63	2.38	1.83
	August	0.60	2.06	1.56	0.66	2.01	1.53
	September	0.61	1.93	1.45	0.70	1.77	1.31
	October	0.66	1.75	1.28	0.71	1.63	1.19
	November	0.59	1.98	1.46	0.60	1.97	1.45
	December	0.58	2.52	1.64	0.66	2.29	1.55
2010	January	0.65	2.19	1.61	0.67	2.14	1.60
	February	0.71	1.81	1.39	0.73	1.77	1.35
	March	0.72	2.01	1.46	0.75	1.92	1.40
	April	0.62	2.29	1.75	0.66	2.22	1.67
	May	0.60	2.12	1.63	0.61	2.09	1.62

were more data proximate in space and time for the spatiotemporal prediction. This resulted in a search neighborhood with denser data, thus reducing prediction uncertainty.

3 Conclusions

By incorporating temporal variability of satellite-observed CO_2, conventional spatial-only geostatistical analysis was extended to a spatiotemporal geostatistical analysis of the satellite-observed CO_2 data in China. The spatiotemporal geostatistical method investigates correlation structure in space and time, and more data are available for stable variogram estimation and prediction relative to the conventional, spatial-only geostatistical method. The potential advantage of the spatiotemporal method is that more significant and accurate geostatistical inferences can be made, because there are more data available in both space and time for

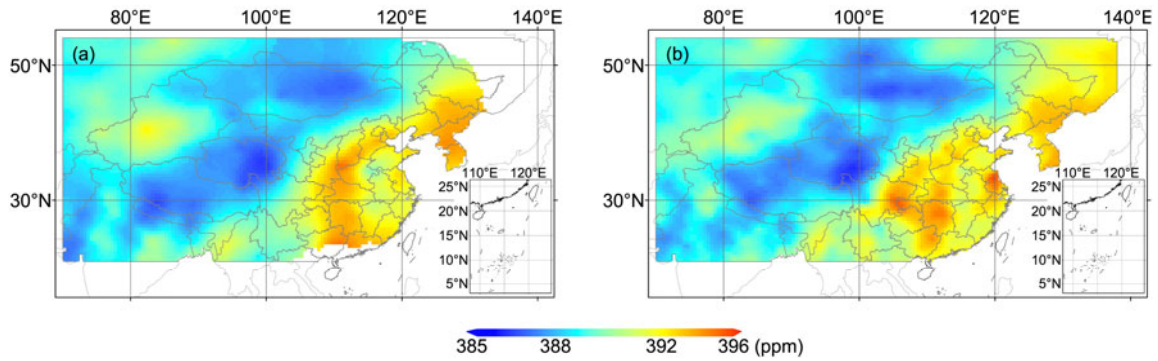

Figure 4 Map of CO_2 predictions for April 2010 in study area using (a) spatial-only, and (b) spatiotemporal geostatistical prediction approaches.

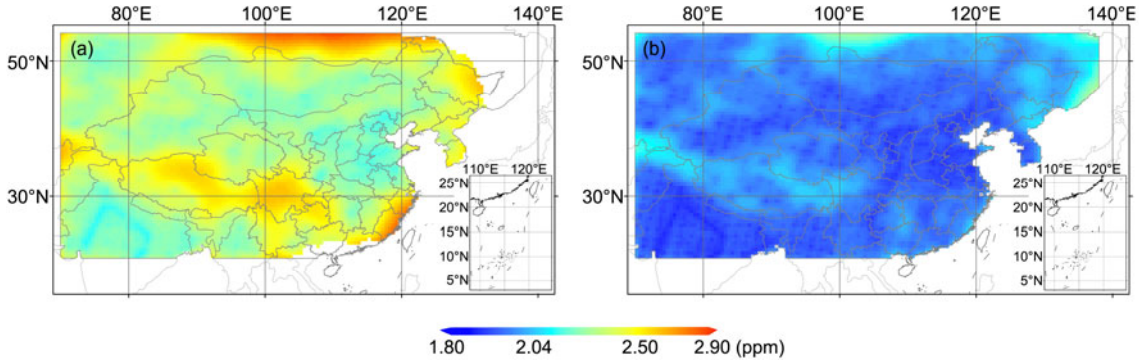

Figure 5 Comparison of prediction standard deviation for April 2010 in study area using (a) spatial-only, and (b) spatiotemporal geostatistical prediction approaches.

prediction. The spatial-only approach needs to partition the full spatiotemporal dataset into monthly data, which may be insufficient in number to obtain a stable estimate of the spatial variogram for each month. Moreover, the temporal structure of the data is ignored in the spatial-only approach.

The spatiotemporal variogram (Figure 3) displayed substantial temporal autocorrelation of CO_2 in China, and it is intuitive that prediction accuracy can be enhanced by incorporating this temporal structure, since more data in both space and time are available for prediction. As a result of prediction assessment using cross-validation statistics, the geostatistical prediction approach based on the estimated spatiotemporal variogram model produced greater prediction accuracy than the spatial-only approach. Moreover, the monthly mapping result of the spatiotemporal approach showed less prediction uncertainty and more detailed spatial variation of CO_2 than those of the spatial-only approach. It is concluded that by incorporating temporal correlation, geostatistical analysis of CO_2 in China may be improved, and the more detailed and precise mapping results could be used for future greenhouse gas study.

The geostatistical prediction methods rely on accuracy of the dataset used, which was the GOSAT XCO2 product in this study. The GOSAT Level 2 data products used here are only retrieved in low aerosol optical depth (<0.5) conditions. In high aerosol optical depth conditions (without CO_2 product), there should be a higher CO_2 mixing ratio because of a stable atmospheric boundary layer structure that limits atmospheric diffusion. Therefore, mapping with consideration of the effect of aerosol optical depth should be done in future studies.

This work was supported by the National Natural Science Foundation of China (41071234) and the Strategic Priority Research Program—Climate Change: Carbon Budget and Relevant Issues of the Chinese Academy of Sciences (XDA05040401). We are greatly grateful to the reviewer and editor for the valuable and excellent comments, and acknowledge the data products provided by NIES GOSAT Project.

1 World Meteorological Organization. WMO WDCGG data summary. WMO WDCGG No. 36, 2012
2 Qian W H, Lu B, Liang H Y. Changes in fossil-fuel carbon emissions in response to interannual and interdecadal temperature variability. Chin Sci Bull, 2011, 56: 319–324
3 Bai W G, Zhang X Y, Zhang P. Temporal and spatial distribution of tropospheric CO_2 over China based on satellite observations. Chin Sci Bull, 2010, 55: 3612–3618
4 NIES GOSAT Project. Algorithm theoretical basis document for CO_2 and CH_4 column amounts retrieval from GOSAT TANSO-FTS SWIR, NIES-GOSAT-PO-017, V1.0, 2010
5 Tomosada M, Kanefuji K, Matsumoto Y, et al. A prediction method of the global distribution map of CO_2 column abundance retrieved from GOSAT observation derived from ordinary Kriging. ICROS-SICE International Joint Conference 2009, Japan, 2009. 4869–4873
6 NIES GOSAT Project. Algorithm theoretical basis document for GOSAT TANSO-FTS L3, NIES-GOSAT-PO-017, V 1.0, 2011
7 Liu Y, Wang X, Guo M, et al. Mapping the FTS SWIR L2 product of XCO_2 and XCH_4 data from the GOSAT by the Kriging method—A case study in East Asia. Int J Remote Sens, 2012, 33: 3004–3025
8 Hammerling D M, Michalak A M, Kawa S R. Mapping of CO_2 at high spatiotemporal resolution using satellite observations: Global distributions from OCO-2. J Geophys Res, 2012, 117: 1–10
9 Tsutsumi Y, Mori K, Hirahara T, et al. Technical report of global analysis method for major greenhouse gases by the World Data Center for Greenhouse Gases. Global Atmosphere Watch Research and Monitoring Report No. 184(WMO/TD No. 1473), 2009. 1–23
10 NIES GOSAT Project. Global greenhouse gas observation by satellite. GOSAT Project, 2012
11 NIES GOSAT Project. Summary of the GOSAT level 2 data product validation activity. GOSAT Project, 2012
12 NIES GOSAT Project. Data processing flow for the FTS SWIR Level 2 CO_2 and CH_4 data products (Version 2.0). GOSAT Project, 2012
13 Cressie N. Statistics for Spatial Data. New York: John Wiley & Sons, 1993
14 Goovaerts P. Geostatistics for Natural Resources Evaluation. New York: Oxford University Press, 1997
15 Heuvelink G B M, Griffith D A. Space-time geostatistics for geography: A case study of radiation monitoring across parts of Germany. Geogr Anal, 2010, 42: 161–179
16 Cressie N, Wikle C K. Statistics for Spatiotemporal Data. New York: John Wiley & Sons, 2011
17 De Iaco S, Posa D. Predicting spatio-temporal random fields: Some computational aspects. Comput Geosci, 2012, 41: 12–24
18 Kyriakidis P C, Journel A G. Geostatistical space-time models: A review. Math Geol, 1999, 31: 651–684
19 De Iaco S, Myers D E, Posa D. Space-time analysis using a general product-sum model. Statist Probab Lett, 2001, 52: 21–28
20 Gething P W, Atkinson P M, Noor A M, et al. A local space-time Kriging approach applied to a national outpatient malaria data set. Comput Geosci, 2007, 33: 1337–1350
21 De Iaco S. Space-time correlation analysis: A comparative study. J Appl Statist, 2010, 37: 1027–1041
22 Jost G, Heuvelink G B M, Papritz A. Analyzing the space-time distribution of soil water storage of a forest ecosystem using spatiotemporal Kriging. Geoderma, 2005, 128: 258–273
23 Cressie N. Fitting variogram models by weighted least squares. Math Geol, 1985, 17: 563–586
24 Arlot S. A survey of cross-validation procedures for model selection. Statist Surv, 2010, 4: 40–79
25 Spadavecchia L, Williams M. Can spatiotemporal geostatistical methods improve high resolution regionalization of meteorological variables? Agr Forest Meteorol, 2009, 149: 1105–1117
26 Chiles J, Delfiner P. Geostatistics: Modeling Spatial Uncertainty. Hoboken: John Wiley, 1999